# Preparation and Characterization of UV-Curable Organic/Inorganic Hybrid Composites for NIR Cutoff and Antistatic Coatings

**Hsien-Tang Chiu, Chi-Yung Chang, Cheng-Lang Chen, Tzong-Yiing Chiang, Ming-Tai Guo**

*Department of Polymer Engineering, National Taiwan University of Science and Technology, Taipei, Taiwan*

Received 5 January 2010; accepted 19 June 2010
DOI 10.1002/app.32978
Published online 13 October 2010 in Wiley Online Library (wileyonlinelibrary.com).

**ABSTRACT:** In this study, UV-curable organic/inorganic hybrid composite coatings with near infrared (NIR) cutoff and antistatic properties were prepared by high-shear mixing of two kinds of polymer matrices and coated on plastic and glass substrates by the doctor-blade method. This study also investigated the morphology, stability, optical properties, electrical resistivity, and durability of the UV-cured composite coats. It was found that the composite coatings were very stable under centrifugation. Moreover, the films with transmittance of above 80% in a visible light region (400–800 nm) and of $\sim$ 40% to 50% in the NIR region (1000–1600 nm) showed low haze of 6.9%, electrical resistivity of around $2.3 \times 10^7$ Ω/square. Thus, excellent adhesion, scratch, and weathering durability can be produced on polycarbonate substrate at room temperature. The experimental results reveal that UV-curable organic/inorganic hybrid composites can be used effectively to fabricate films with NIR cutoff as well as antistatic properties, indicating a high potential for practical application in architectural, automotives, and optoelectronics. © 2010 Wiley Periodicals, Inc. J Appl Polym Sci 120: 202–211, 2011

**Key words:** organic/inorganic hybrid composites; UV-cure; NIR cutoff; antistatic; coatings; stability

## INTRODUCTION

Near infrared (NIR) cutoff coatings are useful in solar energy control and heat protection for increasing energy efficiency in architecture, automotives, and optoelectronics applications.[1,2] For usage of architecture, NIR cutoff coatings can block IR transmit for heat insulation to attain the purpose of energy conservation,[3] similarly to automotives, NIR cutoff coatings can reduce heat conduction to achieve carbon reduction,[4] and, for optoelectronics, NIR cutoff coatings is widely used for display and photovoltaic cells application.[5,6] Various studies have conducting research about how to cutoff NIR spectra as maintaining excellent optical transmission. Among other methods, thin-film metal-oxide coatings have been used commercially as electromagnetic filters for infrared regions for over half a century. Deposition onto substrates has typically been accomplished using vapor deposition techniques[7–9] and more recently, sol–gel methods.[10–12] These coatings provide very good optical performance under abrasion, thermal cycles, and variable humidity when applied on substrates with similar thermal and mechanical properties.

*Correspondence to:* H.-T. Chiu (hchiu@mail.ntust.edu.tw).

Journal of Applied Polymer Science, Vol. 120, 202–211 (2011)


However, when conventional metal oxide coatings are applied to flexible, relatively soft substrates such as polymers, mismatches in mechanical properties can reduce interfacial adhesion or accelerate mechanical failures.[13,14] To overcome these shortcomings, organic–inorganic (O/I) hybrid composite coatings may be the ideal substituent, having both the advantages of the easy application of organic coatings and the analogous functions of inorganic coatings.[15]

Organic/inorganic hybrid composites, in which inorganic and organic components interact at a micro-nanoscale level, have attracted great interest in past years due to resulting synergic properties.[16–19] The hybrid materials obtained possess unique property combinations of the inorganic (hard and brittle) and the organic (soft and flexible), as maintaining optical transparency.[20,21] Most organic–inorganic hybrid network materials reported in previous studies are thermally cured.[22,23] Alternatively, hybrid materials can be prepared through the use of radiation curing using UV-radiation curing systems.[24–26]

UV-curable organic/inorganic hybrid composites are composed of polymer matrices, fillers, and initiators. Pure polymers such as epoxy acrylate (EA) are widely used and significant kinds of UV-curable volatile organic compounds (VOC) coatings. For instance, such polymers bisphenol diglycidylether derivatives can easily be tailored to make coating

products with good adhesion, hardness, and chemical resistance.[27]

Moreover, UV-radiation curing offers a number of advantages which make it particularly well suited for the synthesis of organic–inorganic hybrid composite coatings.[28,29] Because of its very low consumption of energy and its minor emission of VOC,[30] UV-curing technology has become especially attractive, given increasing concern for the environment in industry today.

Until now, however, almost all NIR cutoff coatings have been deposited on glass substrates and thermally cured systems. Very few cases have involved UV-curable organic–inorganic hybrid composites coatings on plastic substrates. Unlike glass substrates, plastic substrates have several advantages over glass substrates, which include robustness, lesser weight, thinness (which provides wide viewing angles), flexibility (for varying the device shape to optimize visibility and thus suppress reflections), durability, and easy scaling-up to large formats for large volume roll-to-roll production.[31–33] The most commonly used substrates are polycarbonate (PC) and polyethylene terephthalate (PET) because of their superior optical properties compared with other polymer substrates.[31] The UV-curable NIR cutoff coatings on plastic films have advantages of low cost and easy manufacturing, superior stability, physical durability, fast curing reactions, and high-energy efficiency.[11,34,35]

Therefore, in this work, because UV-curable organic–inorganic hybrid composite have become more and more important. We attempt to study the properties of UV-curable NIR cutoff organic–inorganic hybrid composite coatings on glass substrate and plastic films (PC, PET), respectively, and their comparisons as well.

In this study, we first prepared two kinds of organic/inorganic hybrid composite coatings by high-shear mixing EC700[36] and CIR-963[37] particles into polymer matrices which consist of appropriate dispersant and polymeric binder. Then the two particles, slurry and photoinitiators were added individually into EA and eventually the two organic–inorganic hybrid composite coatings were prepared, respectively. Finally, we blended the two composite coatings with the appropriate ratios by high-shear mixer to obtain NIR cutoff with antistatic coatings. This study also investigated the optical, surface morphology, durability, and electric properties of the UV-cured composite coats and the stability of the coatings.

## EXPERIMENTAL

### Materials

The powder samples used in the experiment in this study have commercial names. EC-700 as conductive $Al_2O_3$-ITO blue powders (200–300 nm) was purchased from Titan Kogyo, Japan and CIR-963 as NIR cutoff functional aminium compound green powders was obtained from Japan Carlit Co. Trimethylolpropane ethoxylated (6) triacrylate (TMPEOTA) as the function monomer for the EA resin was supplied by Miwon Commercial Co. Polymeric binder, acrylic copolymer type oligomer diluted with diethylene glycol monoethylether (Chemtech-37W-PC-2), and photoinitiator, 2-methyl-1-[4-(methylthio) phenyl]-2-morpholinopropanone-1 (Chemcure-709) were purchased from Chembridge International Co., Taiwan. Polymeric dispersant (solsperse39000) and poly(ethylene glycol monomethyl ether acrylate) (PEGMEA) as solvent was supplied by Lubrizol Co. All materials were used without further purification.

### Methods

#### Preparation of UV-curable organic/inorganic hybrid composites coatings

First, 10 g of photoinitiator was dissolved in 30 g of PEGMEA and then blended with 5 g of dispersant, 4 g of binder, and 50 g of TMPEOTA by high-shear mixer (Charles Ross&Son) for 10 min at 2000 rpm. In this way, the polymer matrices were obtained. Then we added particulate EC-700 (10–30%) into the polymer matrices and the mixture was stirred well by high-shear mixing to break up any agglomerates[38] for 30 min at 3500 rpm. Finally, the UV-curable organic/inorganic hybrid composite coatings were prepared (composite I: with 10 wt %; composite II: with 20 wt %; composite III: with 30 wt %). The preparation of CIR-963 composite coatings was based on a synthesis route as the precursor (composite IV: with 10 wt %; composite V: with 20 wt %; composite VI: with 30 wt %).

Second, we blended together 10 wt % of EC-700 (composite I) and 10 wt % of CIR-963 (composite IV) with the high-shear mixer at 2000 rpm for 30 min to obtain UV-curable NIR cutoff with antistatic organic/inorganic hybrid composites coatings as composite VII. For composite VII, both powders were well dispersed in polymer coating solution. The resultant solution was used for the coating process and the detail is listed in Table I.

#### Fabrication of UV-cured organic/inorganic hybrid composite coats

All organic/inorganic hybrid composite coats (composites I–VII) were prepared by the doctor-blade coating method using a 4-sided applicator (Zehntner GmbH Testing Instruments, Switzerland) on float glass substrates in a thickness of 0.68 mm (Asahi Glass Co., Japan) and a substrate of PC films in a thickness of 0.18 mm (Entire Technology Co.,

**TABLE I**
**UV-Curable Organic/Inorganic Hybrid Composites Coatings**

| Samples/material | EC-700 series | | | CIR-963 series | | | EC + CIR |
|---|---|---|---|---|---|---|---|
| | I | II | III | IV | V | VI | VII |
| TMPEOTA (g) | 50 | 50 | 50 | 50 | 50 | 50 | 50 |
| Binder (g) | 4 | 4 | 4 | 4 | 4 | 4 | 4 |
| Dispersant (g) | 5 | 5 | 5 | 5 | 5 | 5 | 5 |
| PEGMEA (g) | 30 | 30 | 30 | 30 | 30 | 30 | 30 |
| Photoinitiator (g) | 10 | 10 | 10 | 10 | 10 | 10 | 10 |
| Particle content (wt %) | 10 | 20 | 30 | 10 | 20 | 30 | 10 (EC-700 series) + 10 (CIR-963 series) |

Taiwan) and 0.18 mm polyethyleneterephthalate (PET) films (Toyobo Co., Japan), respectively. All substrates were individually rinsed with isopropanol and deionized water for 1 min and air-dried. After each coating step, the coated substrates were dried for 10 min at 110°C and cured by UV irradiation (International Light, USA) with 500 mW/cm$^2$ for 5 min on the coating side.

## Characterizaion

### Morphology observation

The surface morphology of UV-cured composite substrates were characterized by an atomic force microscope (AFM) Multimode TM III (Digital Instruments) and scanning electron microscopy (SEM) JSM-6390 (JEOL).

The UV-cured composite coats were coated using aurum spattering, then observed by SEM.

AFM images of the UV-cured composite coats were taken at room temperature in air and recorded in tapping mode, with a silica probe (NSC 11) and a frequency of 2 Hz. The root square roughness value (Rq) is the standard deviation of the $Z$ values (the height) calculated within the given area as:

$$\mathrm{Rq} = \sqrt{\frac{\sum (Z_i - Z_{\mathrm{ave}})^2}{N}}$$

where $Z_i$ is the current $Z$ value, $Z_{\mathrm{ave}}$ is the average of the $Z$ values, and $N$ is the number of data points within the given area.[39]

### Optical properties

The optical transmission spectrum of the UV-cured substrates were measured by a UV-VIS-NIR spectrometer Lambda900 (Perkin Elmer) using background correction. The scans were collected at 2000 to 250 nm with the speed of 300 nm/min.

Haze was examined with an automatic haze meter TC-HIII DPK (Denshoku) in accord with the ASTM D1003 method.[40] For the ASTM D1003, this is a standard testing method for haze and luminous transmittance of transparent plastics. The haze meter has a measuring area of 10 mm in diameter. It is composed of an integrated sphere, a condenser, a lens, a photo detector, and an ultraviolet C-range light source. The total transmittance (Tt), diffuse transmittance (Td), and haze of the UV-cured composite coats can be measured within given as:

$$\mathrm{Haze} = \frac{\mathrm{Td}}{\mathrm{Tt}} \times 100\%$$

### Stability measurements

Stability measurements of the composite coatings were performed with a separation analyzer LUMisizer LS 6110-58 (L.U.M. GmbH, Germany), which allows to measure the intensity of the transmitted light as function of time and position over the entire sample length simultaneously (measurement scheme see Fig. 1).[41] The sedimentation behavior of the individual samples can be compared and analyzed in detail at constant or variable relative centrifugal force (RCF) up to 2300 $\times$ $g$ by tracing the variation in transmission at any part of the sample or by tracing the movement of any phase boundary. The slope of the sedimentation curves was used to calculate the sedimentation velocity and to assess the stability of the suspensions (RCF = centrifugal acceleration/earth gravity).

Our experiments had the following parameters: volume: 1.4 mL of composite coatings; 3000 rpm time$_{\mathrm{Exp}}$: 12,500 s, $\Delta t$ = 10 s, $T$ = 25°C, Relative Humidity (RH) = 50%. All measurements were repeated and tested at least twice.

### Electrical resistivity measurement

The measurements of electrical resistivity of the UV-cured composite coats were carried out by a two-probe method using a surface resistivity measuring device MCP-HT450 (Mitsubishi Chemical Co.) at room temperature and humidity of 50%.

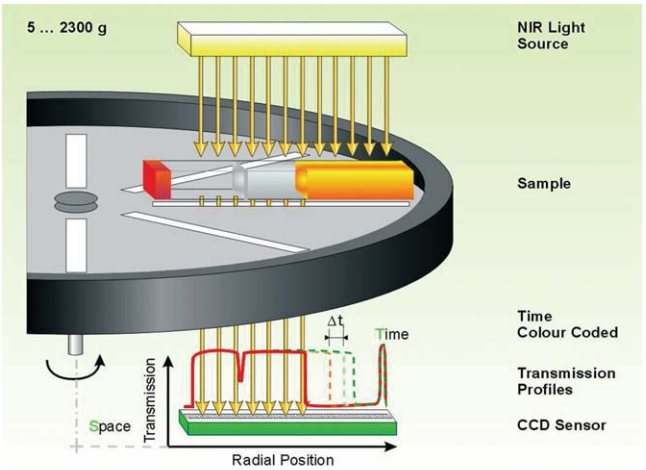


**Figure 1** Measurement scheme of the multisample analytical centrifuge with photometric detection. Parallel NIR-light is passed through the sample cells and the distribution of local transmission is recorded at preset time intervals over the entire sample length. [Color figure can be viewed in the online issue, which is available at wileyonlinelibrary.com.]

### Durability investigation

The scratch resistance (termed as pencil hardness thereafter) of the coating was characterized by a commercial pencil hardness tester (Scratch Hardness Tester Model 291, Erichsen Testing Equipment). The test conforms to ASTM Standard D3363,[42] where a vertical force of 7.5 ± 0.1 N was applied at 45° angle to the horizontal film surface as the pencil is moved over the coated specimen. The grades from the softest to the hardest are: 6B-5B-4B-3B-2B-B-HB-F-H-2H-3H-4H-5H-6H-7H-8H-9H.

The adhesion was evaluated by the crosshatch cutter method using Zehntner Cross-cut tester No. 2087 (Zehntner GmbH Testing Instruments) in accordance with the ASTM D3359.[43] For ASTM D3359, a lattice pattern with 11 cuts in each direction is made in the film to the substrate. Pressure-sensitive tape is placed over the lattice and then removed, and adhesion is evaluated by comparison with descriptions.

The accelerated weathering test was carried out for 336 h using a UV Condensation Weathering Device UV2000 (ATLAS) in accordance with ASTM G154.[44] The UV-cured composite coats were exposed to UVA 340 fluorescent lamps with an irradiation level of 0.77 W/m$^2$. After completion of the exposure cycle, the coats were tested for transmission to ascertain the effect of treatment.

## RESULTS AND DISCUSSION

### Stability of UV-curable organic/inorganic hybrid composite coatings

The stability of the dispersed composite coatings in the polymer matrices was investigated by the sedimentation method using a special centrifuge with an integrated optoelectronic sensor system, which allows for recording of the spatial and temporal changes of light transmission during rotation.[45] Throughout the measurement, transmission profiles were recorded and the sedimentation process was characterized by the time-dependent displacement of the relative position of the boundary between the supernatant and sediment. The transmission profiles were integrated in the middle position (100–110 mm) and displayed these values versus the centrifugation time results in the curves as shown in Figure 2. The transmission value at time $t = 0$ indicates the initial value of transmission which is not related to the stability of dispersion. The change in integral transmission versus time is directly related to the dispersion stability and the sedimentation rate. A low-initial slope indicates a low-sedimentation rate during the measurement corresponding to high stability of the dispersion.[41] The sedimentation rate of particles in solution of composited system can be defined as:

$$V_{\text{sed}} = \frac{2r^2\Delta\rho}{9\eta}a$$

where $r$ is the particle radius, $\Delta\rho$ is the density difference between particle and polymeric solution, $a$ is centrifugal force, and $\eta$ is the viscosity of the polymeric solution. Because the centrifugal force is constant for a given cell geometry and rotation rate, the sedimentation velocity can be influenced by particle size, density, or viscosity with differences between particles and solution. The initial slopes of the integral transmission for composites I and II, composites IV and V, and composite VII were very low. Those composite coatings were very stable under centrifugation.

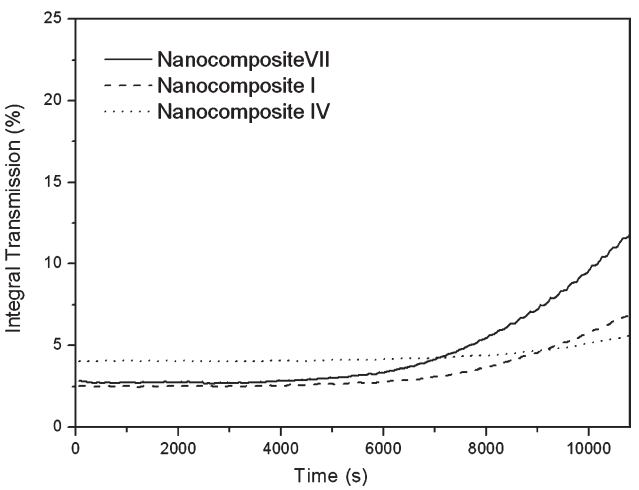


**Figure 2** Integral transmission of organic/inorganic hybrid composites coatings.

As seen in Figure 2, the integral transmission of composites I and IV shows excellent stability with lower initial slopes among others. The curves of composites II and V display slight ascent at 2 h compared with composites I and IV. It is because that the particle content of composites II and V is much more than composites I and IV. The more particles content the more particle–particle interaction. Therefore, the particles collide with each other easily cause the agglomeration of particles. The agglomerations lead to the instability of coatings. Similarly, the composites III and VI show extremely unstable because of the particles agglomeration. Additionally, the composite VII shows an increase of the transmission values from 3 up to 10 (%). The integral transmission curve exhibits a rapid increase of up to about 2 h which resemble the composites II and V; however, starting at 2 h, the integral transmission increases with a higher slope indicating two-step sedimentation as shown in Figure 2. It can be assumed that, after this time, agglomerates of EC-700/CIR-963 were formed and that these agglomerates settled faster. This demonstrates that the stability of composite VII is dependence on the interaction of EC-700 and CIR-963 and it exhibits low-initial slope result in great stability.

### Optical properties of UV-cured organic/inorganic hybrid composite coats

Experiments have accomplished the fabrication of composite coatings to obtain UV-curable coats. In this study, coatings consisting of different concentrations of powders (composites I–VII) were coated on glass substrates and the transmission spectrums for the coatings were measured over wavelengths between 250 and 2000 nm. The results of the transmission spectrums are shown in Figure 3. From Figure 3(a), it is evident that the EC-700 coats (composites I–III) maintain high transmission of over 80% from wavelength 250 and 2000 nm. In other words, the transmission of EC-700 coats is almost unaffected by an increase in EC-700 concentrations, thus the transmission value remains at an average of $\sim$ 84% in the visible light region (400–800 nm). For CIR-963 coats (composites IV–VI) from Figure 3(b), one can see that the rapid decrease in transmission between 750 and 1250 nm depends on the absorption of CIR-963[37] in the NIR region. The two drops at about 1000 and 1520 nm of 50% and 66.9% transmittance, respectively, as well as the gradual lowering of transmission at 1520 nm is due to the increase in CIR-963 concentrations.

The coated PC and PET films in comparison with coated glass substrates show variations in transmission spectra in Figure 4(a–c). It is apparent that composite IV still shows surprising results in cutoff

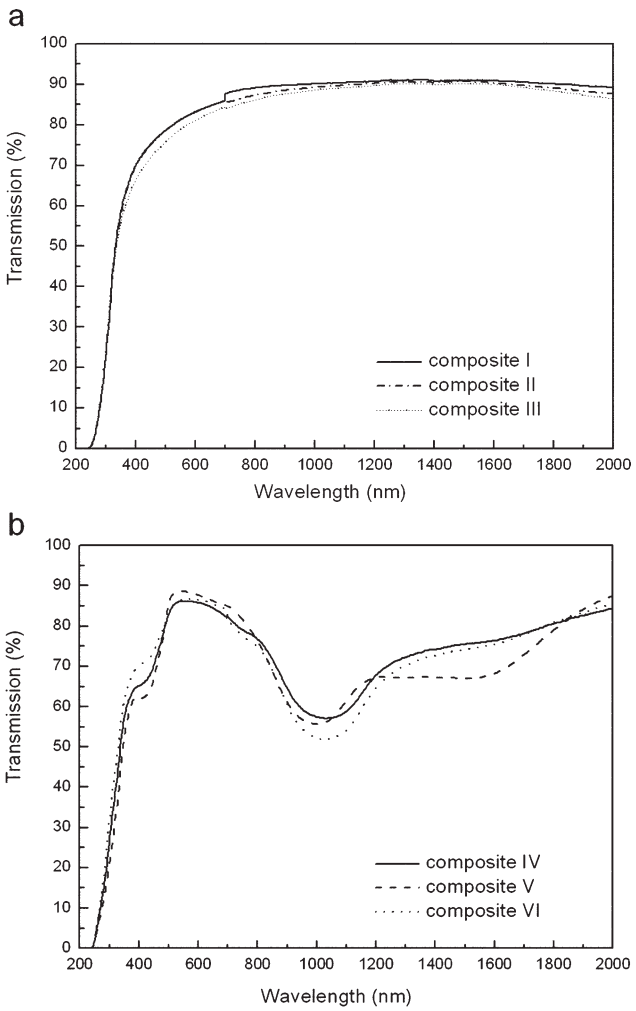


**Figure 3** Transmission spectra of UV-cured organic/inorganic hybrid composite coats on glass substrates: (a) Composites I–III and (b) composites IV–VI.

wavelength of optical transparency between 800 and 1700 nm in the NIR region on plastic substrates. Moreover, composite I maintain high transmittance of $\sim$ 83% between 250 and 2000 nm on plastic substrates. As shown in Figure 4(c), the transmission spectra of composite IV coated on PC film exhibits the minimum value of transmission on the curve of transmissions comparing substrates at about 30% at 1000 nm and 35% at 1600 nm.

For glass/plastic coated substrates, the effect of cutoff wavelength in the NIR region of the coated PC film is obviously greater than the others. From Figure 4, we can see that the composite coatings show good compatibility with both glass and plastic substrates, even the effect of NIR cutoff of on coated plastic films is better than with the coated glass substrates given in Figure 4(b,c).

The results of haze measurement as a function of the coated glass, PC, and PET substrates are given in Figure 5. Figure 5 shows that variation of haze value for coated substrates is observed with a haze

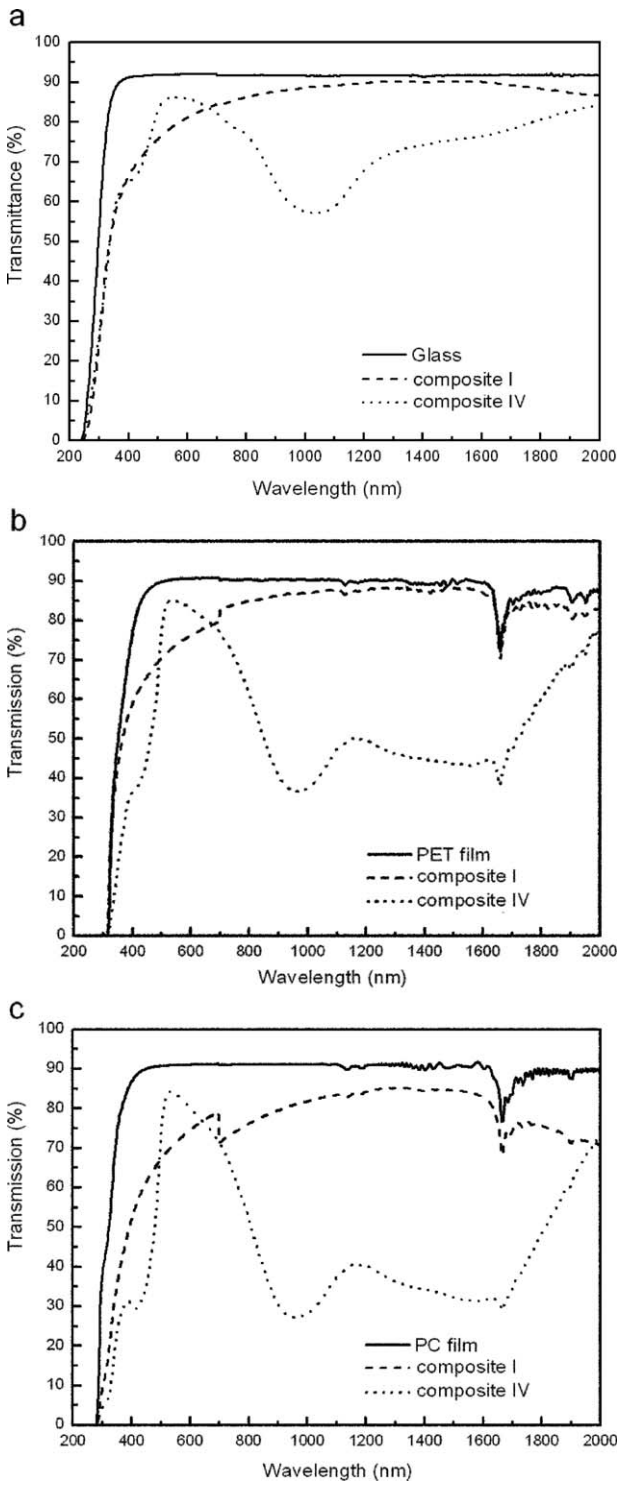


**Figure 4** Transmission spectra of UV-cured organic/inorganic hybrid composite coats (I and IV) on different substrates: (a) Glass, (b) PET, and (c) PC.

of about 0.3% (glass), 0.5% (PET film), 0.7% (PC film) for composite IV and 3% (Glass), 3.5% (PET film), 3.7% (PC film) for composite I. For composites I and IV, there is no notable difference in the haze measurement of the various coated substrates. From wavelengths of 400 to 800 nm in the transmission

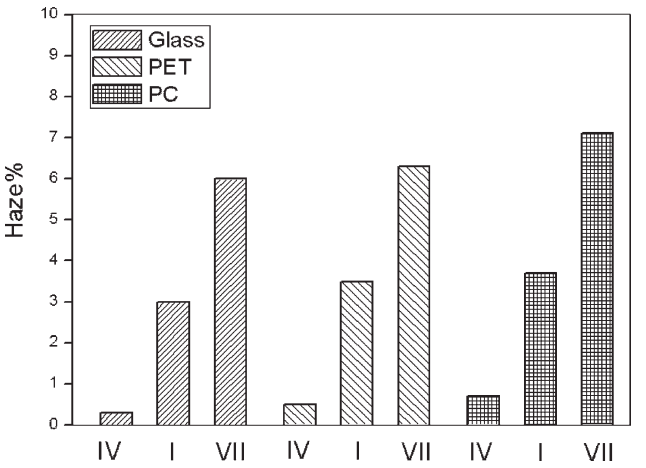


**Figure 5** Variations of haze value of UV-cured organic/inorganic hybrid composite coats with different substrates.

spectra, the transmissions of the coated substrates maintain high value, corresponding to low value in haze measurement. Therefore, it is very evident that composites I and IV coatings on plastic/glass substrates exhibit high transparency in the visible light region.

### Optical properties of UV-cured antistatic NIR cutoff coats

To obtain high transparency with NIR cutoff and antistatic coatings, we mixed composites I and IV together thoroughly by high-shear mixing. Then, the blended coating (composite VII) was used to fabricate NIR cutoff coats with antistatic characteristics as described above. The transmission spectra of composite VII on glass, PET, and PC substrates are given in Figure 6.

Figure 6 shows wavelength curves descending and ascending between 750 and 1250, and also at

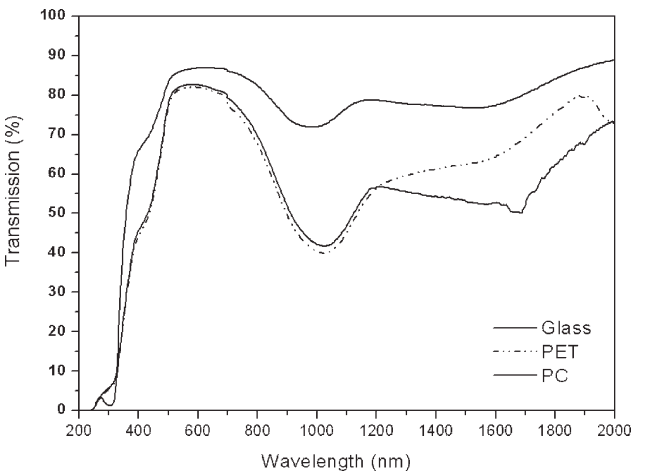


**Figure 6** Transmission spectra of UV-cured antistatic NIR cutoff coats.

about 1600 nm. By comparing overall figures from the NIR region, composite VII on PET and PC film shows transmittance of ~ 40% at a wavelength of 1100 nm. Moreover, the coated PC film exhibits an average of 50% between 1200 and 1750 nm. In contrast with the transmission of composite VII, with composites I and IV, there are no distinct variations in the visible light region. Furthermore, composite VII maintains NIR cutoff characteristics. Figure 6 shows that composite VII of different substrates exhibit haze of about 6% (glass), 6.3% (PET film), and 7.1% (PC film). These results indicate low and indifferent haze levels for composite VII on plastic films compared with glass substrates. In other words, the fabrication of the NIR cutoff and antistatic coats on plastic films show high clarity and lower haze. In addition, composite VII on PC film has been found to exhibit high transparency in visible light regions with low haze and good efficiency for NIR cutoff characteristics. As follows, the surface morphology, surface resistivity, and durability of coated PC film will be described below.

### Surface morphology of UV-cured antistatic NIR cutoff coats

SEM images of composite VII on different substrates are shown in Figure 7. Surface roughness was determined by atomic force microscopy (AFM). The results are given in Figure 8. From Figure 7(a) of composite VII coated on PC film, one can see that the particles show good dispersion in the organic matrix although some aggregates are still evident. The particles are loosely irregular with a size of about 200 nm formed by the aggregation with partial uniformity resulted in the surface roughness (Rq) of about 174 nm as shown in Figure 8(a). The composite VII coated on PET film [Fig. 8(b)] from which the aggregations still occur, however the degree of aggregation is less than the composite VII coated on glass substrate and the surface roughness (Rq) of about 146 nm [Fig. 8(b)]. Hardly any aggregation happens in the SEM of composite VII coated on glass substrate [Fig. 7(c)]. Furthermore, the surface roughness (Rq) of about 110 nm exhibited in Figure 8(c), in contrast to coated PC and PET film, the coated glass substrate is smooth and less roughness. Additionally, we compare the results of the surface roughness (Rq) and haze measurement, more the coated surface is rough more the haze value is high. For coated PC film, the surface roughness is 174 nm with haze of 7.1% and the coated glass substrate show the surface roughness is 110 nm with haze of 6%. The haze increases monotonously with increasing roughness.

Although the surface roughness of the composite film should be attributed to homogenous dispersion, however, somehow the interaction between either the EC-700/CIR-963 or EC-700/CIR-963/polymer matrices may cause aggregation resulting in the rough surface on the coated films.

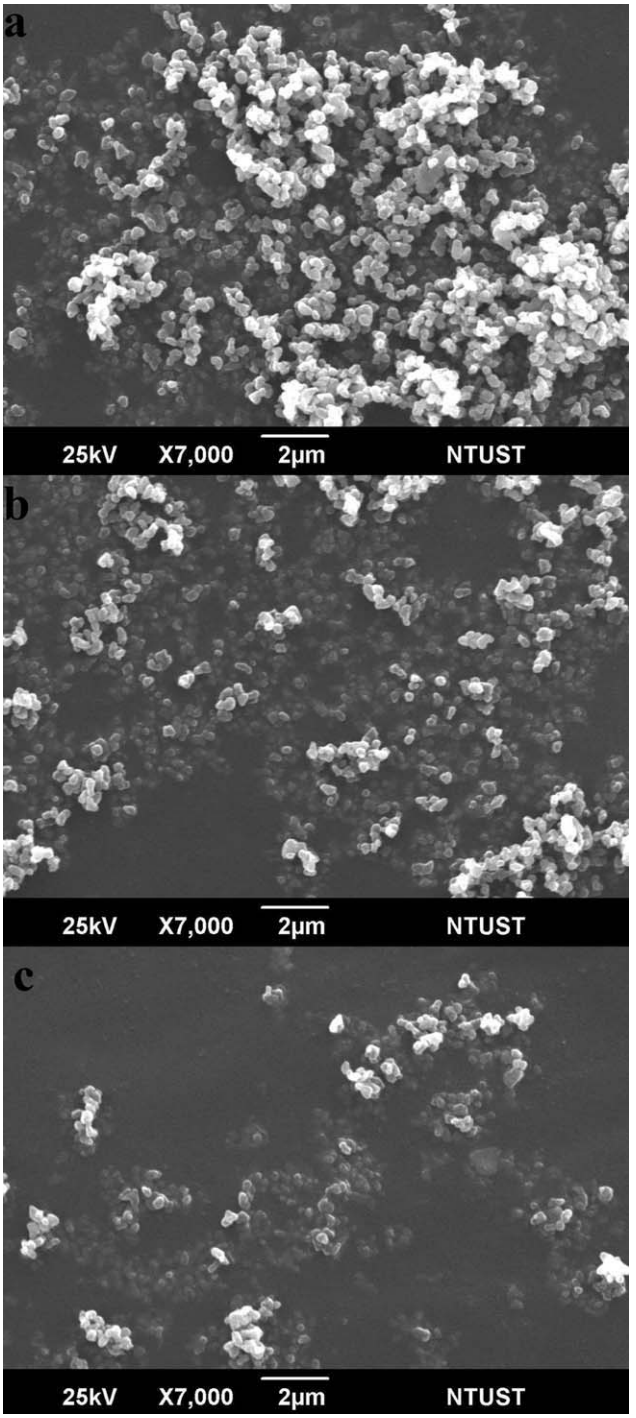


**Figure 7** SEM images of UV-cured antistatic NIR cutoff coats on different substrates: (a) PC, (b) PET, and (c) glass.

### Electrical properties of UV-cured antistatic NIR cutoff coats

The surface resistivity of composite VII on PC film decreases with the increasing content of EC-700.

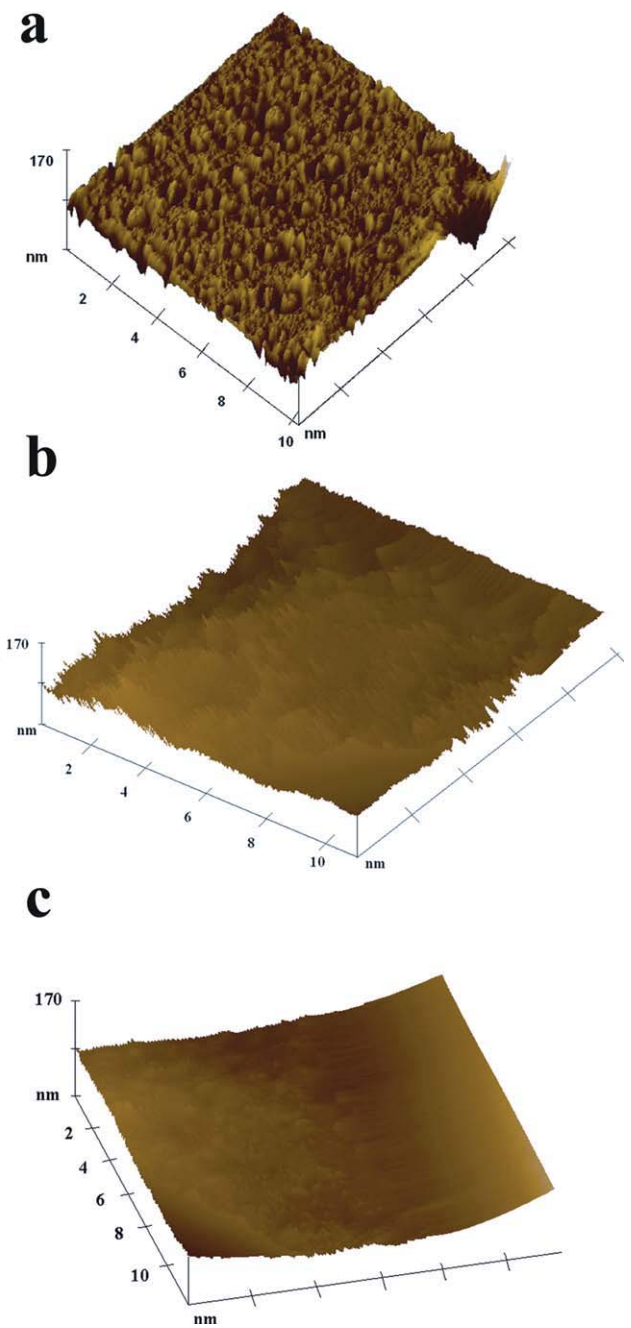


**Figure 8** AFM images of UV-cured antistatic NIR cutoff coats on different substrates: (a) PC, (b) PET, and (c) glass. [Color figure can be viewed in the online issue, which is available at wileyonlinelibrary.com.]

This result was obtained by the surface resistivity measuring device shown in Table II. This figure shows the coats contain 10 wt % of EC-700 (composite I) with $2.3 \times 10^7$ Ω/square and 30 wt % with $1.82 \times 10^5$ Ω/square (composite III). We obtained the antistatic properties by using coatings containing 10 wt % of EC-700 (composite I) to fabricate antistatic properties instead of 30 wt % (composite III) due to the increase of EC-700 content caused by the high haze in the coated substrates. However, the

**TABLE II**
**Variations of Surface Resistivity with EC-700 Concentration**

| EC-700 concentration | Surface resistivity (Ω/square) |
|---|---|
| 10% | $2.3 \times 10^7$ |
| 20% | $2.87 \times 10^6$ |
| 30% | $1.82 \times 10^5$ |

coatings contained 10 wt % of EC-700 (composite I) and possessed antistatic characteristics with high transmittance in the visible light area (average of 80%) as shown in Figure 6. The surface resistivity of the coatings was higher than the surface resistivity of pure EC-700 particles ($10^1$ to $10^3$ Ω/square), this should be attributed to the barrier role of the polymer phase and the dispersant against electron transfer.

### Durability of UV-cured antistatic NIR cutoff coats

The scratch resistance of the composite VII coats is determined using a calibrated set of drawing pencils

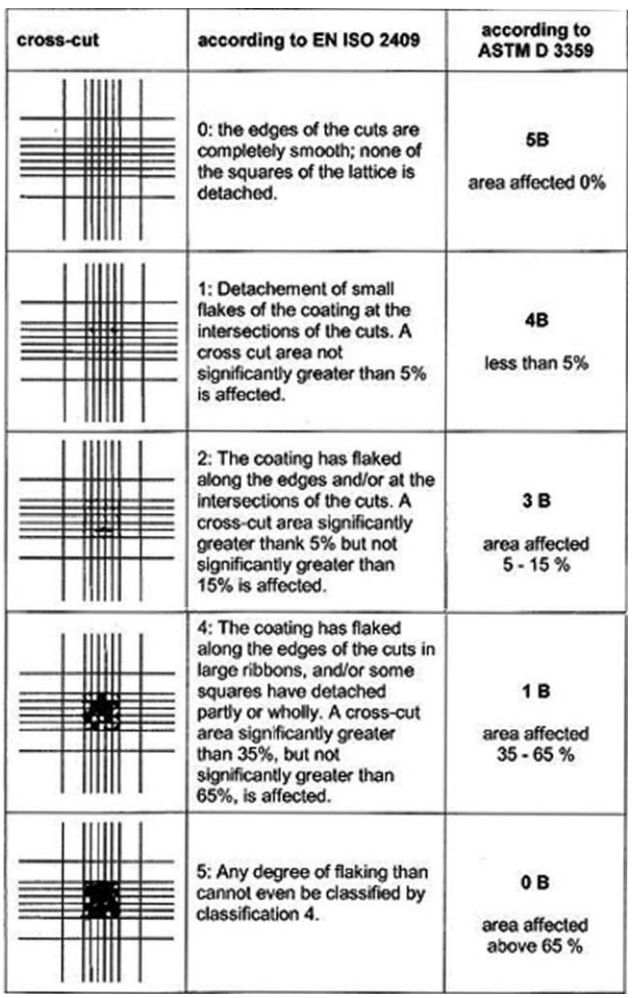


**Figure 9** Classification chart of standard adhesion scale according to ASTM D3359.

**TABLE III**
**The Scratch and Abrasion Resistance of Composite VII Coating on Different Substrates**

| Substrates | Coating thickness (μm) | Scratch resistance | Abrasion resistance |
|---|---|---|---|
| Glass | 9.3 | 4H | 5B |
| PC | 9.5 | 3H | 5B |
| PET | 8.9 | 3H | 5B |

that range from 9B, the softest, to 9H, the scratch resistance of the uncoated PC film was Hard black (HB), PET film for 2H and glass substrate for 8H. The scratch resistance of coated films with composite VII was 3H-4H, the scratch resistance increased for both coated PC and PET films but decreased for glass substrate. This can be attributed to coating thickness on films is adequate to prevent substrate plowing, which caused the scratch failure[46]; this confirms the effectiveness of the scratch resistance of original composite VII coatings.

The abrasion resistance of composite VII coats is determined by the adhesion and the roughness of the coats. Excellent adhesion was measured by cross-cut and tape test. The coating tests were conducted in accordance with ASTM D3359[43] (Standard test methods for measuring adhesion by tape test method A: the X-cut test) using 3M Scotch 610 tape. According to the scale in the standard as shown in Figure 9, the coatings all have a 5B level value: the edges of the cuts are completely smooth; none of the squares of the lattice are detached. The results of scratch resistance and abrasion resistance are shown in Table III.

For further characterization of composite VII on PC film, a long-term UV-exposure was performed, according to ASTM G154.[44] After the long-term UV test (336 h), almost no change in the transmission spectra could be detected within the error of measurement as shown in Figure 6; therefore, the filters exhibit extremely good wear resistance at room temperature. From these results, the good durability of composite VII on PC film is attributed to the very good adhesion and wear resistance of the coated layer.

## CONCLUSIONS

The UV-curable organic/inorganic hybrid composite coats allow for the preparation of a NIR cutoff filter with antistatic properties by using the doctor-blade coating method on plastic films with composite VII coatings, which consist of polymer matrices/EC-700/CIR-963 composite. Furthermore, the organic/inorganic hybrid composite coating (composite VII) shows good stability under centrifugation. Moreover, it was found that the optical properties of the coated PC film shows $\sim$ 80% visible transmittance between 400 and 800 nm and 40% of transmission spectra in the NIR region between 1000 and 1600 nm. In addition, we can observe low haze of about 6.9% and excellent durability to the adhesion of the 5B level value, and scratch of 3H value as well as good wear resistance. Room-temperature surface resistivity give around $2.3 \times 10^7$ Ω/square, which leads to antistatic character. Therefore, with these preliminary results, we anticipate that the organic/inorganic hybrid particles EC-700/CIR-963-based UV-curable polymer coatings with excellent optical properties and high stability will open up new perspectives for various applications, because sufficient performance and reduced costs can be expected. The ongoing work is directed toward the investigation of the effects of enhancing inorganic–organic ratios of UV-curable NIR cutoff composite coatings on refractive index, optical loss, and birefringence of optical properties for optical waveguides.

## References


1. Berning, P. H. Appl Opt 1983, 24, 4127.
2. Sechar, S. C. Energy Build 1998, 28, 307.
3. Lampert, C. M. Sol Energy Mater 1981, 6, 1.
4. Turler, D.; Hopkins, D.; Goudey, H. SAE 2003, 1, 1076.
5. Lee, J.-H.; Lee, S.-H.; Yoo, K.-L.; Kim, N.-Y.; Hwangbo, C. K. Surf Coat Technol 2002, 158, 477.
6. Dehu, C.; Jian, X.; Ting, Z.; Paradee, G.; Ashok, S.; Gerhold, M. Appl Phys Lett 2006, 88, 183111.
7. Glocker, D. A.; Shah, S. I. Handbook of Thin Film Process Technology; Institute of Physics: London, 1995.
8. Waits, R. K.; Vossen, J. L.; Kern, W. Thin Film Processes; Academic Press: San Diego, 1978.
9. Martinu, L.; Poitras, D. J Vac Sci Technol A 2000, 18, 2619.
10. Chen, K. M.; Sparks, A. W.; Luan, H. C.; Lim, D. R.; Wada, K.; Kimerling, L. C. Appl Phys Lett 1999, 74, 3805.
11. Mennig, M.; Oliveira, P. W.; Frantzen, A.; Schmidt, H. Thin Solid Films 1999, 351, 225.
12. Thomas, I. M. Proc SPIE 1994, 232, 2114.
13. Grego, S.; Lewis, J.; Vick, E.; Temple, D. Thin Solid Films 2007, 515, 4745.
14. Rhee, Y. W.; Kim, H. W.; Deng, Y.; Lawn B. R. J Am Ceram Soc 2001, 84, 1066.
15. Sanchez, C.; Julián, B.; Belleville, P.; Popall, M. J Mater Chem 2005, 15, 3559.
16. Avella, M.; Errico, M. E.; Martuscelli, E. Nano Lett 2001, 1, 213.
17. Haas, K. H.; Schwab, S. A.; Rose, K. Thin Solid Films 1999, 351, 198.
18. Wouters, M. E. L.; Wolfs, D. P.; Linde, M. C.; Hovens, J. H. P.; Tinnemans, A. H. A. Prog Org Coat 2004, 51, 312.
19. Wen, J. Y.; Wilkes, G. L. Chem Mater 1996, 8, 1667.
20. Mackenzic, J. D.; Bescher, E. J Sol-Gel Sci Technol 2003, 27, 7.
21. Latella, B. A.; Ignat, M.; Barbe, C. J.; Cassidy, D. J.; Barlett, J. R. J Sol-Gel Sci Technol 2003, 26, 765.
22. Chiang, C. L.; Ma, C. C. M. J Eur Polym 2002, 38, 2219.
23. Chou, T. P.; Chandrasekaran, C.; Limmer, S. J.; Seraji, S.; Wu, Y.; Forbess, M. J.; Nguyen, C.; Cao, G. Z. J Non-Cryst Solids 2001, 290, 153.

24. Buestrich, R.; Kahlenberg, F.; Popall, M.; Dannberg, P.; Muller, R.; Fiedler, R.; Rösch, O. J Sol-Gel Sci Technol 2001, 20, 181.
25. Innocenzi, P.; Brusatin, G. J Non-Cryst Solids 2004, 333, 137.
26. Soppera, O.; Croutxe-Barghorn, C.; Carre, C.; Blanc, D. Appl Surf Sci 2002, 186, 91.
27. Chattopadhyay, D. K.; Siva, S. P.; Raju, K. V. Prog Org Coat 2005, 54, 10.
28. Decker, C. Prog Polym Sci 1996, 21, 1319.
29. Decker, C. Macromol Rapid Commun 2002, 23, 1057.
30. Bayramoğlu, G.; Kahraman, M. V.; Kayaman-Apohan, N.; Güngör, A. Prog Org Coat 2006, 57, 50.
31. Cairns, D. R.; Paine, D. C.; Crawford, G. P. In SID'01 Digest, Society of Information Display 2001, p 654.
32. Lueder, E. Proc SPIE 1998, 64, 3297.
33. Suo, Z.; Ma, E. Y.; Gleskova, H.; Wagner, S. Appl Phys Lett 1999, 74, 1177.
34. Hoyle, E. C.; Kinstle, F. J. Handbook of Radiation Curing of Polymeric Materials; American Chemical Society: Washington, DC, 1990.
35. Latoska, P. N. J Coat Technol 1995, 67, 27.
36. Nakatani, H. (to Zeon Corporation) U.S. Pat. 570,151 (2007).
37. Kuwabara, S. U.S. Pat. 883,920 (2005).
38. Bardin, M.; Knight, P. C.; Seville, J. P. K. Powder Technol 2004, 110, 169.
39. Xiong, M.; You, B.; Zhou, S.; Wu, L. Polymer 2004, 45, 2967.
40. ASTM. Standard test method for haze and luminous transmittance of transparent plastics, ASTM D 1003; ASTM, USA, 2003.
41. Lerche, D. J Dispersion Sci Technol 2002, 23, 699.
42. ASTM. Standard test method for film hardness by pencil test, ASTM D 3363, ASTM, USA, 2005.
43. ASTM. Standard test methods for measuring adhesion by tape test, ASTM D 3359, ASTM, USA, 2006.
44. ASTM. Standard practice for operating fluorescent light apparatus for ultraviolet exposure of nonmetallic materials, ASTM G 154, ASTM, USA, 2000.
45. Sobisch, T.; Lerche, D. Colloid Polym Sci 2000, 278, 369.
46. Chen, Z.; Linda, Y. L. W.; Edmund, C.; Tham, O. Mater Sci Eng A 2008, 493, 292.